Article

Indoor Localization System Based on Bluetooth Low Energy for Museum Applications

Romeo Giuliano [1,*][iD]**, Gian Carlo Cardarilli** [2]**, Carlo Cesarini** [1][iD]**, Luca Di Nunzio** [2,*]**, Francesca Fallucchi** [1]**, Rocco Fazzolari** [2][iD]**, Franco Mazzenga** [3]**, Marco Re** [2][iD] **and Alessandro Vizzarri** [3]

[1] Department of Innovation & Information Engineering, Guglielmo Marconi University, via Plinio 44, 00193 Rome, Italy; carlo.cesarini@gmail.com (C.C.); f.fallucchi@unimarconi.it (F.F.)
[2] Department of Electronics Engineering, University of Rome "Tor Vergata", Via del Politecnico 1, 00133 Rome, Italy; g.cardarilli@uniroma2.it (G.C.C.); rocco.fazzolari@uniroma2.it (R.F.); marco.re@uniroma2.it (M.R.)
[3] Department of Enterprise Engineering "Mario Lucertini", University of Rome "Tor Vergata", Via del Politecnico 1, 00133 Rome, Italy; mazzenga@ing.uniroma2.it (F.M.); alessandro.vizzarri@uniroma2.it (A.V.)
[*] Correspondence: r.giuliano@unimarconi.it (R.G.); di.nunzio@ing.uniroma2.it (L.D.N.)

check for updates

Abstract: In the last few years, indoor localization has attracted researchers and commercial developers. Indeed, the availability of systems, techniques and algorithms for localization allows the improvement of existing communication applications and services by adding position information. Some examples can be found in the managing of people and/or robots for internal logistics in very large warehouses (e.g., Amazon warehouses, etc.). In this paper, we study and develop a system allowing the accurate indoor localization of people visiting a museum or any other cultural institution. We assume visitors are equipped with a Bluetooth Low Energy (BLE) device (commonly found in modern smartphones or in a small chipset), periodically transmitting packets, which are received by geolocalized BLE receivers inside the museum area. Collected packets are provided to the locator server to estimate the positions of the visitors inside the museum. The position estimation is based on a feed-forward neural network trained by a measurement campaign in the considered environment and on a non-linear least square algorithm. We also provide a strategy for deploying the BLE receivers in a given area. The performance results obtained from measurements show an achievable position estimate accuracy below 1 m.

Keywords: bluetooth low energy; indoor localization system; received signal strength indicator; neural network

1. Introduction

Accurate estimation and tracking of the positions of people, objects or animals enables the provisioning of several advanced services such as the automatic execution of task(s) triggered by events consisting for example of a person passing a specific position in the area, commercial or recreational applications requiring location information inside a specific area, etc. [1]. In the last few years, the possibility of realizing advanced communication applications and services supported by position information have favored and encouraged the development of systems for the indoor localization of people and objects. In parallel, the evolution of these systems has been constantly supported by the technological advancements of internet of things (IoT) [2] technologies specifically conceived for low-cost short-range radio transmission such as Bluetooth [3] and its variants and radio frequency identification (RFID) technologies [4].

The design of localization systems based on short range radio technologies is not a trivial task. In fact, radio signal propagation inside buildings is influenced by several factors, such as construction

materials, objects in the area, the presence of people, etc. All these factors can influence the quality of the received signal, thus rendering indoor localization very complex and expensive when it is directly based on the measurements of physical parameters of the received signals from the person/object to be localized. Unlike for outdoor navigation, which is mainly based on global navigation satellite system (GNSS) technologies (e.g., the Global Positioning System, GPS), to date indoor positioning systems have not yet been defined or standardized. The lack of standardization is mainly due to the very different characteristics of the areas to be served by the indoor localization system. As a consequence, this localization system is often specifically designed for the area, making use of heterogeneous, diversified, and very often customized position calculation techniques and processes.

In the last years, the use of machine learning (ML) algorithms has been proposed in several applications such as health [5,6], communication [7,8], energy [9,10], etc. This has been possible thanks to two main reasons: (i) the availability of big data introduced by the internet, and (ii) the increasing computational capability of circuits and microprocessors. ML also plays an important role in IoT systems. Nowadays, in many applications, the data acquired by IoT nodes are transmitted over the internet and processed on remote servers provided by ML algorithms. Thus, these servers can analyze and interpret the data and provide predictions of the system behavior.

Unfortunately, this strategy requires the transmission of all the data collected by the sensors. This aspect is in many cases a big limitation. For example, consider all those cases in which the transmission of this data requires non-negligible data rates. In these cases, in order to ensure the correct transmission of all data, it is not possible to use low power wireless technologies, thus limiting the battery life of the sensor nodes. Moreover, having ML in IoT sensors allows the reduction of the computational load of the remote server, since part of the computation is performed locally.

In the future, thanks to a mix of new technologies and design methodologies that allow the processing of data more and more efficiently both in terms of computational power and power consumption [11–13], it is possible to imagine that ML algorithms will be moved closer and closer towards the nodes' sensors in order to process data locally and transmit only a small amount of information to the internet with consequent energy savings and longer battery life.

In this paper we focus on the localization problem for a typical museum environment. The availability of position information from the visitors in the museum can be used by the museum operator to advance communication services aiming at improving the overall "cultural experience". In particular, position information can be helpful for the museum operator to design art exhibitions, to define personalized itineraries in accordance with visitor preferences, permanent, or temporary installations, and to take care of the collections. All these activities can be based on the analysis of visitor flows, for example, by observing the number of visitors stopping in front of a given artwork or the amount of time spent in some areas inside the museum. In addition, the estimates of the positions of visitors can be exploited to facilitate/improve their interaction with the museum artworks in real time, for example, by means of augmented reality providing information on the artwork they are observing at a given moment. In the latter application case, each visitor is equipped with a smart device (e.g., his/her smartphone or tablet) including a device to communicate with the indoor localization system and able to interact with museum indoor applications providing, for example, additional information on the observed/enjoyed masterpiece/artwork [14]. The localization system presented in this paper can be deployed in environments other than the museum, such as shopping malls, large offices, indoor parking, and train stations or airports.

The considered system exploits Bluetooth Low Energy (BLE) technology to collect data transmitted by the device owned by each visitor. The main advantages of BLE are large chipset availability on the market and on modern smartphones/tablets, ease of programming, and low energy consumption. The resulting BLE-based localization system is low-cost when compared to other indoor positioning techniques such as those based on (non-standard) RFID devices. In the considered localization system, BLE signals emitted by the visitor's transmitters are received by the BLE devices installed in the museum area. These devices can measure the received signal strength indicator (RSSI) and the

signal-to-noise ratio (SNR) of each received signal and can extract the identity of the BLE transmitter by retrieving the associated message. The measured RSSI and SNR and the corresponding BLE message are then passed to a central server in the museum. The locator entity in the server processes the received data and messages to extract the position of the visitor in the museum. The localization algorithm of each visitor is based on the minimization of an objective function including the pathloss measurements obtained from the associated RSSIs and SNRs. The optimal solution to the minimization problem corresponding to the estimated position of the visitor is obtained by applying a non-linear least square (NLS) algorithm. At the end of this paper, we also analyze the problem of the deployment of the BLE receiver in a given area. Results show that a BLE transmitter can be localized with an accuracy lower than 1 m (i.e., the Euclidean distance between the true and estimated position is lower than 1 m) when the BLE receiver is properly deployed in the area.

Due to difficulties in estimating the wireless channel by modeling its behavior in indoor environment through classical power law trends, we performed a measurement campaign in a typical museum space, used to train a neural network. This allowed us to avoid the fingerprinting of the entire area, which is time-consuming and loses accuracy in the next phase when people are present in the environment. Moreover, it allowed us to take into account the physical characteristics of the environment (e.g., materials, reflection, diffraction), which is usually difficult to model. After the neural network training, the BLE receiver can better estimate the distances based on the RSSI and SNR measurements collected during visitor movement around the artworks.

Here, we report the main contributions of this paper to the topic of localization in indoor environments:

- The preparation phase (performed offline) is based on a non-invasive measurement campaign in the considered space where people are going to be localized. The offline phase in most papers can be long and costly (see below) [15,16]. In our case it consisted of collecting RSSI values between the receiver and the transmitter in a few positions in the area, with the aim of gaining knowledge of the propagation environment and the involved mechanisms (e.g., scattering and reflections);
- Unlike some works in the literature (such as [17–20]; see Related Works section) where the distance estimation was expressed by evaluation of the radio frequency signal attenuation and its related pathloss model (i.e., model-based positioning), we introduced a neural network trained by the measurements collected in the preparation phase. This allowed us to overcome the problem of estimating the distance based on propagation distance and radio signal strength, which may give very complex results in indoor environments;
- We analyzed different deployment strategies in the considered area by evaluating the positioning errors in terms of the deployed scenarios. Differently from [21], in this analysis we gained an indication of how many receivers should be deployed, and where;
- Finally, unlike other methods proposed in the literature such as fingerprinting (such as in [22,23]), we performed an analysis where possible human obstruction could occur during the normal phase. This is important since other studies have failed in position estimation because their RSSI collection was done without any human presence, which means results are different when people obstruct the RF signal.

The paper is organized as follows. In Section 2, related works on this topic are discussed. In Section 3, the principal scheme of the system architecture is detailed. In Section 4, the testbed for the measurement campaign is described and the neural network adopted for the distance estimation is detailed. In Section 5, the localization procedure and the corresponding localization algorithm are explained. In Section 6, the performance results of the considered localization system are reported in terms of the achievable accuracy with the density of BLE receivers in the area installed by the museum operator. Finally, conclusions are drawn.

2. Related Works

Indoor positioning is a well-studied topic in the current literature [1,24]. The proposed localization systems have been based on different strategies/algorithms for deriving positioning information. Some of them have presented limitations in terms of deployed infrastructure, precise environmental characterization, and the costs of the equipment. As an example, positioning methods based on a pathloss fingerprint dataset of the area as in [22] require lengthy preparation for the collection of fingerprints. This can be difficult to achieve especially when the area under consideration is very large such as museum spaces, making the proposed system independent from the size of the environment. Moreover, the relationship between the RSSI and the estimated channel model is difficult to obtain due to multipath, reflections and scattering mechanisms occurring in the area.

Other systems have used the direction of the signal (angle of arrival, AoA) or time of arrival of the signal (time of arrival, ToA) [25] for the localization. For this purpose, the use of antenna arrays is mandatory, especially for AoA measurements. Furthermore, ToA adoption requires time synchronization between the transmitting and receiving devices. This leads to an increase in the complexity and costs of the localization system. In addition, non-line of sight (NLoS) propagation conditions lead to a worsening of accuracy for the position estimate. Other positioning systems have been based on recursive optimization procedures for the position estimate [26] leading to a delay in the calculation.

BLE-based localization systems were illustrated in [27]. Unlike the system presented in this paper, they did not consider in detail the important aspect concerning the transfer of information from the BLE receivers to the centralized server. In the system presented in the present paper the asynchronous protocol Message Queue Telemetry Transport (MQTT) [28] was used. It allows message distribution to be performed very quickly, while minimizing traffic over the network. This results in more efficient communication, reduced response times and allows improvement of the tracking feature. Furthermore, the proposed system allows the estimation of the distance between the receiver and transmitter based on the neural network and the direct application of the localization algorithm, making the whole process simpler and faster. Finally, the adoption of BLE technology allows the localization or tracking of not only high performing devices such as smartphones but also low-cost IoT devices, maintaining reliability and accuracy without requiring particular hardware components or specific and costly synchronization functionalities.

In [23], the authors proposed using recurrent neural networks for wireless fidelity (Wi-Fi) fingerprinting based on RSSI for indoor localization. Their effort was limited to corridors and the neural network estimation was not accurate in the presence of other people, due to the fact that fingerprinting is collected without people. To reduce the time-consuming procedure of performing fingerprinting in an area, the authors in [29] proposed training a long short-term memory recurrent neural network but limiting the algorithm to the considered trajectories of people. In [30] the authors proposed a technique to detect the presence of a human body blocking the RSSI reception in a dynamic environment. The authors applied an artificial neural network for the compensation of RSSI values. In contrast, in [30], we considered not just one single person obstructing the RSSI, but an entire group of visitors. In [17] the authors presented a localization method based on the classical power-law behavior of RSSI. This paper did not consider the effect of obstacles in the relationship between RSSI and distance. In addition, this method was realized for an outdoor environment; [18] is affected by the same limitation. The method proposed in the paper did not estimate the real channel function of the environment and it was tailored to a specific environment. The parameters used for distance estimation were correlated with a specific room and are not easy to generalize. The method proposed in [15] presented two limitations: the training procedure is very long, and it is not clear how the localization method would perform in the presence of other people in the same room. The method proposed in [31] needed the localized person to be equipped with a smartphone since their algorithm exploited the fusion of sensors embedded in the mobile device. This limits the applicability of the localization due to vendor-dependent sensors. The work proposed in [32] seems to be very interesting but the authors did

not provide information in terms of accuracy (the error in meters was not presented). The localization technique presented in [21], similarly to [31], required the use of Android smartphones or tablets. Another limitation of this work is that the authors did not analyze any deployment strategy for the BLE access points. In [19] the authors presented a localization procedure based on the estimation of the channel model by classical power laws. Such a technique provides accuracy in the order of 5–20 m for technologies such as Wi-Fi at 2.4 GHz and at 5 GHz, and BLE at 2.4 GHz. This level of accuracy and that in [33] are not compatible with a museum scenario. The approach proposed in [16] implies a very complex and slow training phase. It requires 5000 samples every 4.5 min with the necessity of many receiving BLE devices. In addition, such a system has been tested on a narrow corridor characterized by reduced position uncertainty. In addition, the authors did not analyze performance in the presence of more than one person in the environment. Finally, the work proposed in [20] was based on the power law and the authors did not analyze the performance in the presence of human obstacles.

3. System Architecture

Figure 1 reports the environment of the proposed BLE-based localization system and its possible deployment in a museum [34].
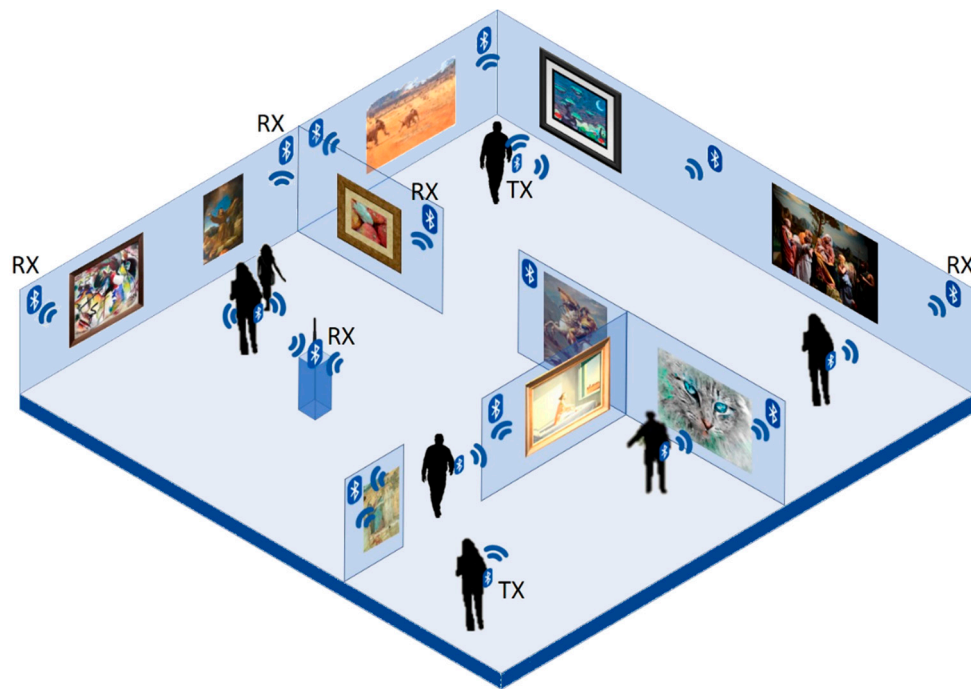

Figure 1. Typical museum environment with the localization of devices.

The architecture of the proposed system highlighting its components is depicted in Figure 2.
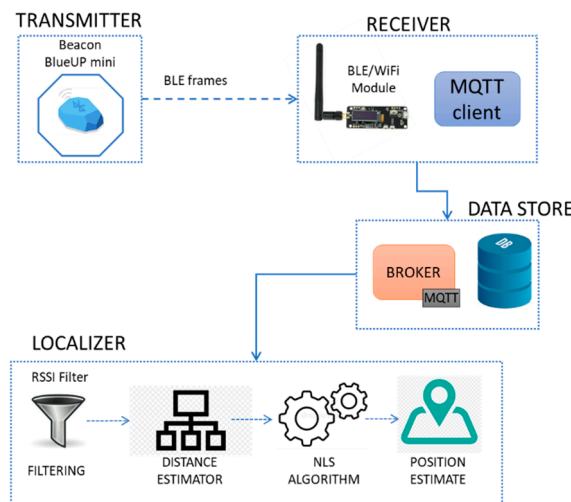
Figure 2. Principal scheme of the considered localization system.

We assume that the object/person to be localized and (possibly) tracked is equipped with a BLE device. This transmits BLE frames at regular time intervals. A number of BLE receivers are (intelligently) installed by the museum authority in the visiting area and they measure the RSSI and the SNR of the received signals and extract the associated BLE messages. Depending on the specific position of the BLE receiver, the RSSI and the identity (ID) of the visitor in the BLE message are transmitted to a centralized server using Ethernet and/or Wi-Fi links.

In our practical implementation, each BLE receiver is equipped with a MQTT client, which provides the MQTT broker with the collected data. The broker forwards data to the central server, where they are first stored and then processed so to discard outliers. As shown in the following section, RSSI and SNR data can be used to estimate path loss and the visitor's position.

The BLE transmitter typically operates in the advertising mode to transmit information. Figure 3 reports the BLE advertising Protocol Data Unit (PDU) indicated in the Bluetooth standard [35]. In the same figure we also indicate the packet formats corresponding to three popular advertising applications currently available in the market [36] i.e., Apple's iBeacon, the AltBeacon open format from Radius Networks, and Google's Eddystone. In this work, we have considered the Eddystone UID format. This consists of a unique code, which can be used to identify visitors or specific categories of objects/people. The Eddystone format defines four types of frames: unique ID (UID) frames, ephemeral ID (EID) frames, URL frames, and telemetry (TLM) frames.
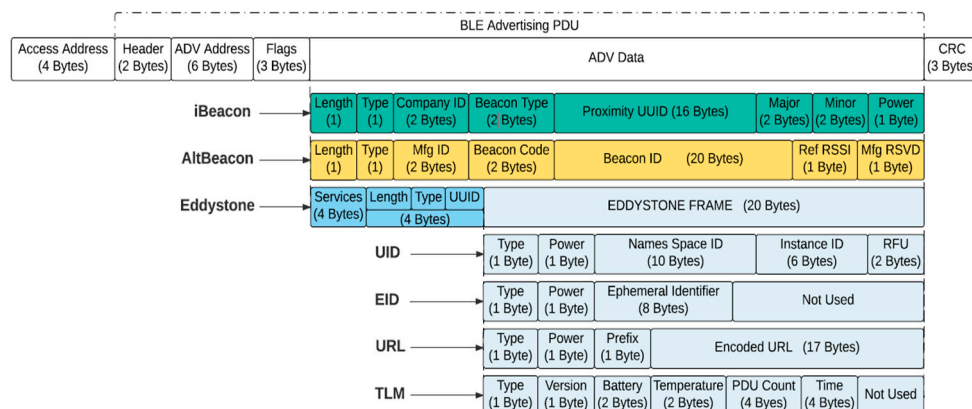

Figure 3. iBeacon, AltBeacon and Eddystone frames [17].

4. Propagation Model Estimation in the Considered Environment

In order to evaluate the effectiveness of the proposed system in providing the localization service in a museum, we developed a testbed to characterize the antenna behavior in the considered environment and to perform a measurement campaign for the training of the neural network. In particular, we considered receivers equipped with two different types of antennas: an integrated antenna and an external antenna with a gain of 5 dBi. In this section, we describe the testbed setup, the radiation pattern of the two receiving antennas, and the neural network definition.

4.1. Testbed Setup

In the testbed we used two devices: the ESP32-WROOM-32D equipped with an integrated antenna and the ESP32-WROOM-32U equipped with an external antenna of 5 dB gain [37,38]. ESP32-WROOM-32D and ESP32-WROOM-32U are generic Wi-Fi + Bluetooth + BLE microcontroller modules that target a wide variety of applications, ranging from low-power sensor networks to the most demanding tasks, such as voice encoding, music streaming and MP3 decoding. Thanks to the dual mode, each receiver is allowed to receive packets on the BLE link and transmit them over the Wi-Fi link, reported in Figure 4a.
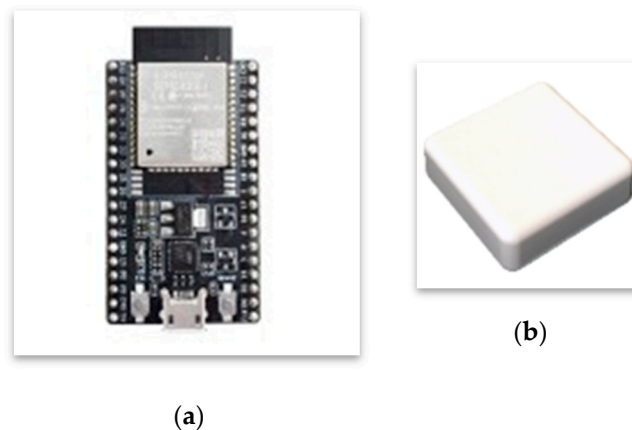

(**b**)

(**a**)

Figure 4. (**a**) Receiver; (**b**) transmitter.

The transmitter beacon was a "BlueUp mini", which is Google-certified and compliant with the BLE standard, reported in Figure 4b. It is very small in size (40 mm × 40 mm × 15 mm) and it is equipped with an nRF51822 Nordic chip. The management software allows the definition of different configurations such as transmission interval, transmission power, and frame format. The battery has a long life (from 6 months to 5 years). For the testbed we adopted the following setup: Eddystone frame UID format, a transmission time interval of 500 ms, and a transmission power (TxPower) of -4 dBm. The packet contained the information necessary to measure the RSSI.

Both receivers were programmed to acquire the advertising packets via BLE transmitted by enabled beacons. For the transmission from the receivers to the central server we used the MQTT protocol [28] on the Wi-Fi link. MQTT is a simple and light communication protocol based on the publish/subscribe paradigm; it is asynchronous and therefore suitable for data transmission between IoT devices. The broker receives data in JavaScript Object Notation (JSON) format.

The data were stored in a relational SQL Server database, which simplified the analysis and processing operations on the received RSSI values.

In Figure 5 we report the setup of the testbed used to characterize the antenna of the two receivers (Figure 5a) and to perform the measurement campaign (Figure 5b).
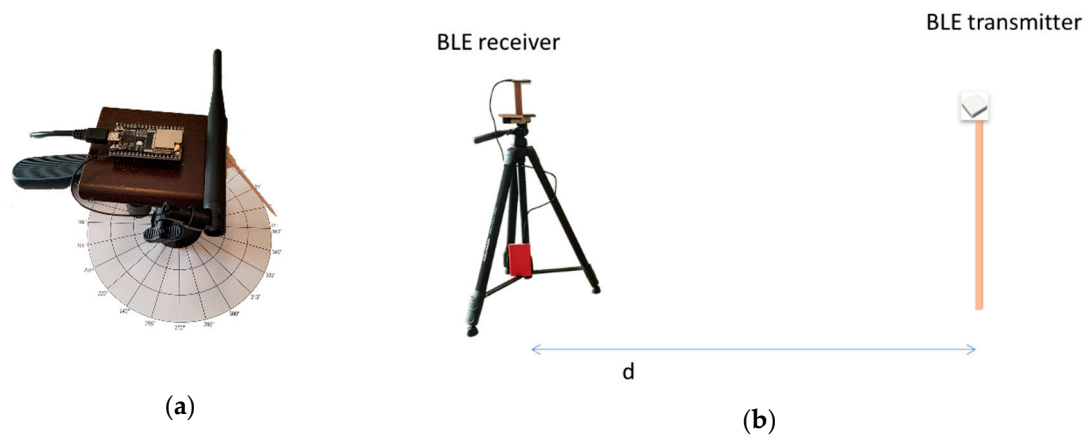
Figure 5. Testbed used for the measurement campaign and for the characterization of the antennas: (**a**) BLE receiver; (**b**) equipment for pathloss measurements as a function of the distance d.

4.2. Measurement Campaign

In order to characterize the radiation pattern of the receiving antennas and to collect proper indications for training the neural network, we placed the transmitter in the center of the considered environment. Then, we positioned the receivers (one a at time) in four directions (namely north, west, south, and east with respect to the transmitter) and at different distances from the transmitter. The positions of the receivers and the transmitter are showed in Figure 6.
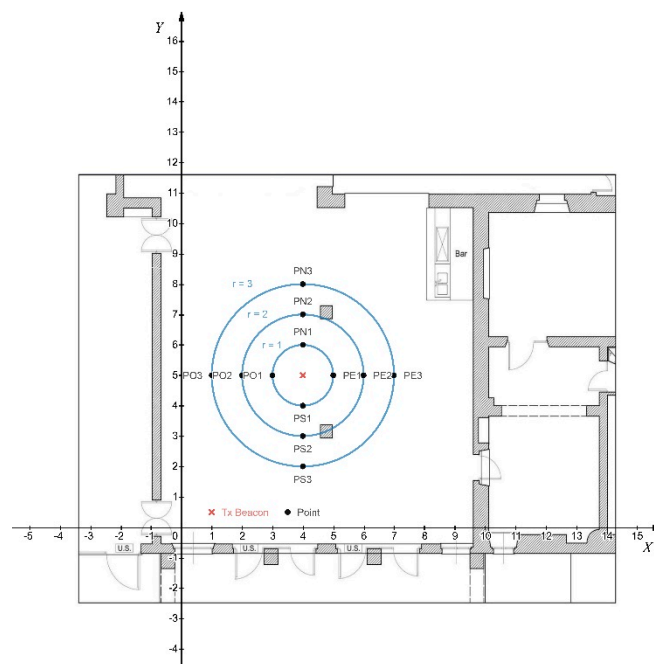

Figure 6. Environment and positions used to characterize the radiation pattern of the antennas.

Each measurement was based on the transmission of 150 UID Eddystone frames. For each received frame, the RSSI value was stored in the database. These values were raw and needed to be processed to limit the fluctuations accounting for the variability of the wireless channel. This filtering process was based on two steps. First, the values were averaged. Then, values exceeding the average plus/minus the standard deviation were identified and discarded, since they are considered outliers [39]. Other filtering strategies can be considered [40]. A measurement sample set is reported in Figure 7a, while Figure 7b reports its probability density function (PDF).
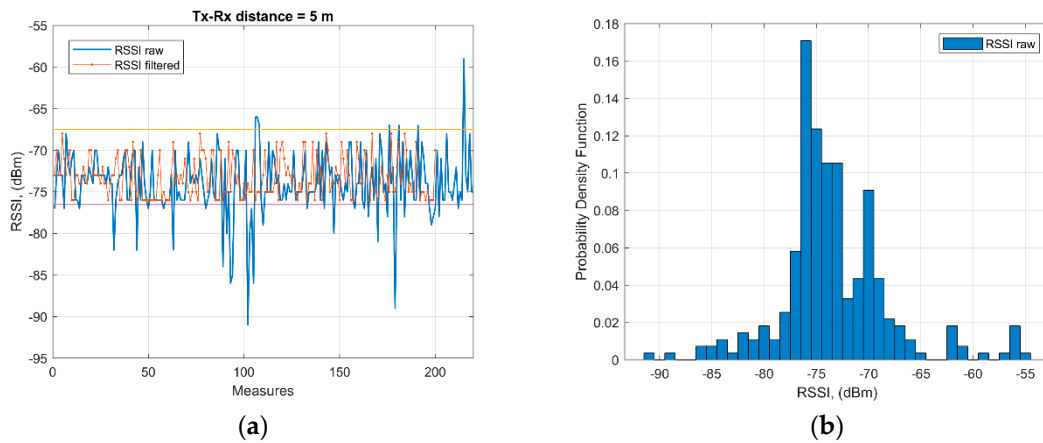
(a)

(b)

Figure 7. Measurement example at 5 m: (**a**) RSSI values for 200 received frames; (**b**) probability density function (PDF) of received RSSI.

4.3. Radiation Diagram Evaluation

The procedure for the measurement campaign to evaluate the radiation pattern of the two considered antennas is reported as follows:

1. The receiver was placed at a distance of 1 m north with respect to the transmitter.
2. 150 RSSI values were acquired at $0°$, $90°$, $180°$, and $270°$ by rotating the receiver on its position in the directions north-east-south-west. Thus, a total of 600 values were acquired in the north direction.
3. Point 2 was repeated in the east, south, and west directions with respect to the transmitter.

Then, at a distance of 1 m, 2400 RSSI values were acquired in total. Points (1) to (3) were repeated at distances from 2 m to 5 m. After the acquisition phase, the values were then filtered, thus excluding outliers, i.e., values greater than the average (at a given distance and for a given direction) plus the standard deviation and lower than the average minus the standard deviation in the considered position.

The results of the receiver with the internal antenna are reported in Figure 8a,b at distances of 2 and 5 m, respectively.
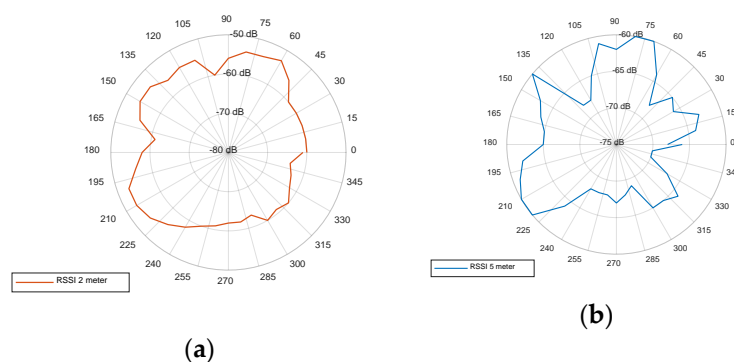

(a)

(b)

Figure 8. Receiver with internal antenna at: (**a**) 2 m; (**b**) 5 m.

The results of the receiver with the external antenna are reported in Figure 9a,b at distances of 2 m and 5 m, respectively.
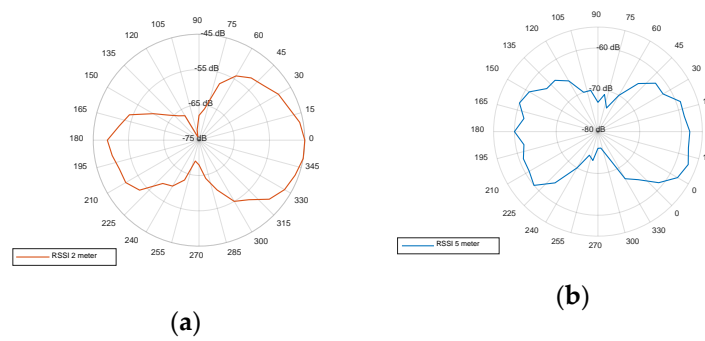
Figure 9. Receiver with external antenna at: (**a**) 2 m; (**b**) 5 m.

With reference to the radiation diagram, identified for both receivers, it can be noted that the receiver with integrated antenna, under a certain distance, maintained omnidirectional radiation, while the receiver with external antenna had a higher gain with a narrower radiation beam offering excellent coverage with beam width of +60° to −60° in the north/south direction.

As an example, in Figure 10 we report the results of measures ranging from 1 m to 3 m. The correlation between the average received RSSI and the measured direction can be highlighted. In this case, we used the receiver with the internal antenna.
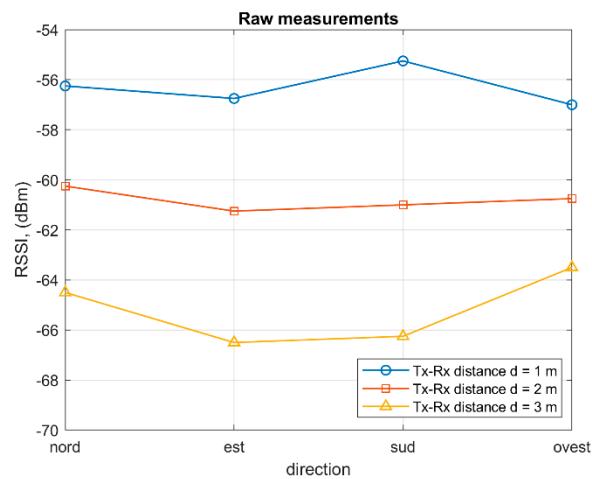

Figure 10. Correlation between RSSI and direction.

4.4. Neural Network for Distance Estimation

In the following, we report the theoretical equations aiming to describe the physical behavior of the communication system between the transmitter and receivers. In order to estimate the distance between them, we express pathloss as a function of the measured RSSI and SNR, whose Equations are reported in (1) and (2), respectively:

$$RSSI = P_R + N \tag{1}$$

$$SNR(d) = \frac{P_R(d)}{N} \tag{2}$$

where N is the received noise power of the receiver and P_R is the received power. Its expression is reported in (3):

$$P_R(d) = \frac{P_T G_T G_R}{L(d)} \tag{3}$$

where P_T is the transmitting power, and G_T and G_R are the gain of the transmitter and receiver antennas, respectively. By evaluating N in (2) and substituting it into (1), after some algebra we can explicit the pathloss L(d):

$$L(d) = \frac{P_T G_T G_R}{RSSI(d)} \cdot \left(1 + \frac{1}{SNR(d)}\right) \tag{4}$$

Due to the very short distances between the BLE transmitter and the receivers in the museum we can assume that RSSI is equal to the received power, i.e., SNR is high, and that noise power is negligible.

The modeling of the pathloss as a function of the distance between the transmitter and the receiver is difficult to obtain even when a massive measurement campaign is provided. This is due to the fact that the signal behavior follows reflection, diffraction and scattering mechanisms, especially in an indoor environment. Moreover, a complete campaign should be performed extensively in each environment where the localization system is deployed. To overcome the difficulties in environment characterization, we performed a relatively fast measurement campaign in the museum spaces. As explained below, this is different from performing a very time-consuming measurement campaign in the whole museum (or in the generic area where the localization service is provided). Our measurements are based on a limited test, which are then used to train the neural network, with the aim of characterizing the environment where the localization system is deployed.

We performed measurements according to the scheme reported in Figure 11. Starting from the reference distance d_0 equal to 1 m, we collected frames at 17 points. The first 6 points were spaced by 0.5 m, while the rest of the points were at a distance of 1 m from each other. As previously, we collected 150 RSSI values for each distance. For each distance, we rotated the receiver in four directions: north, west, south and east, with respect to the transmitter. Again, in this case, outliers were discarded.
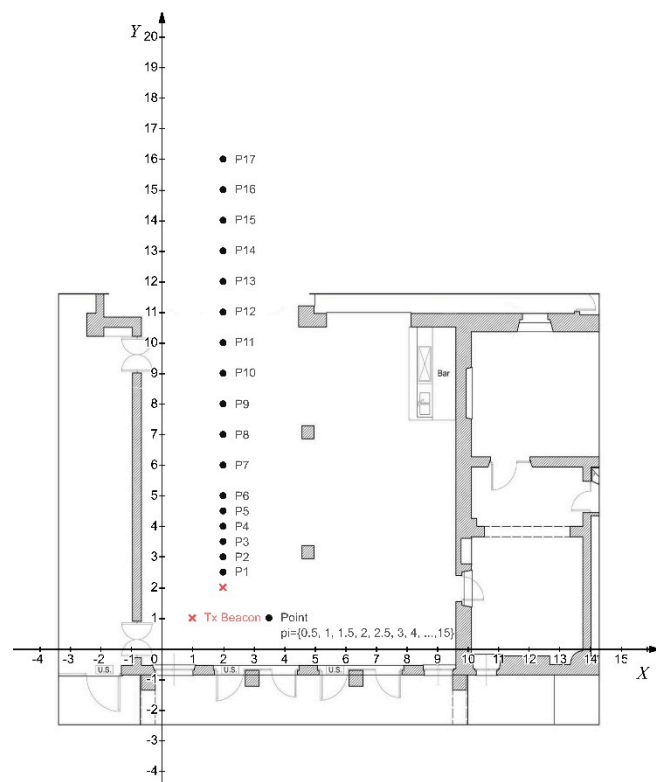

Figure 11. Measurement campaign for neural network training.

For the fitting of the distance estimation function, we used a two-layer feed-forward neural network: one hidden layer and one output layer. The hidden layer was composed of ten neurons with a sigmoid activation function. The output layer consisted of a single neuron with a linear activation

function. The neural network was been trained with the scaled conjugate gradient backpropagation algorithm. The training of the neural network was performed by providing the RSSI received by the single beacon as the input vector and the distance between the transmitter and the beacon as a target vector. Both the training and the design of the neural network were performed in MATLAB. The resulting neural network was converted into the C++ language using the MATLAB coder, in order to be implemented in the receiver board.

Figure 12 reports the output of the neural network for receivers with both external and internal antennas. In the same figure, RSSI measurements and their average are reported as a function of distance. Due to local propagation mechanisms (e.g., multipath, reflections, scattering, etc.) characterizing the environment, the relationship between RSSI and the distance between the transmitter and the receiver can be difficult to estimate and it is often far from the monotonic behavior of the typical power-law propagation models. The neural network tries to fit as much as possible with the behavior of the radio signal in the considered environment based on the RSSI measurements.
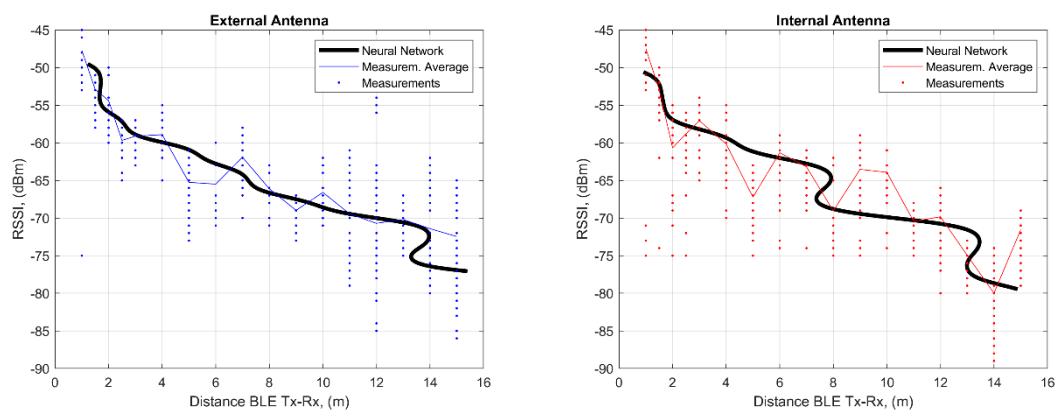

Figure 12. Neural network fitting and RSSI measurements for receiver with external (**left**) and internal (**right**) antennas as a function of the distance.

5. Localization Procedure

In this section, we provide the description of the localization procedure proposed in this paper. It was based on the preliminary phase for the distance estimation in the considered environment and the characterization of the transmitter and receiver antennas. The procedure was based on the reception of three or more BLE receivers placed in the room to be monitored, i.e., where transmitters needed to be localized in the museum in order to provide a greater user experience to visitors as well as to improve the museum management. When the server is able to collect data from more than three receivers because the distance and the propagation conditions allow it, the localizer should select the best receivers for the localization. This is necessary since we observed that an increase in receivers introduces higher noise in the estimation phase.

The following reports the localization procedure:

1. The transmitter starts to transmit frames with the set transmission power and the set frequency. This value is fixed (and known by the localizer) in the environment where the localization service is provided.
2. For each receiver in the room that receives frames (i.e., the distance between the transmitter and the receiver is such that the SNR is above the threshold), it collects $N_X = 5$ frames (i.e., a measurement set).
3. For each measurement set, the receiver filters the data and the neural network estimates the distance between the transmitter and the receiver.
4. The receiver sends the pair of estimated distances to the server.

5.　The localizer in the server sorts the array with the estimated distances and selects the three shortest distances.

6.　The localizer applies the NLS algorithm to these distances and estimates the position of the transmitter.

The complete formulation of the NLS algorithm is in [41]. Figure 13 reports a flowchart of the localization procedure.
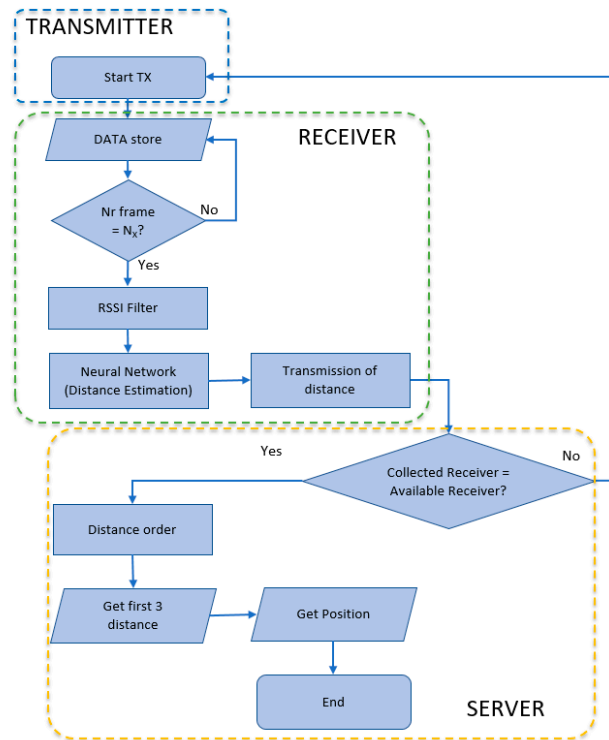

Figure 13. Flow chart of localization procedure.

6. Experimental Setup

6.1. Performance Evaluation of the Distance Estimator

In order to evaluate the position and the number of BLE receivers to be deployed in the considered area to be monitored, it is necessary to analyze the errors in real distance with respect to the estimated distance between the transmitter and the receiver evaluated according to the neural networks. In Figure 14, we report the distance error between the real position in Figure 11 and the neural network-estimated position. The error was less than 2 m for a distance of 9 m for receivers with both internal and external antennas. For higher distances the error increased to 4 m for the external antenna receiver and to 6 m for the internal antenna receiver. In the same figure, we also reported the distance error obtained using the theoretical pathloss model in (4) $L(d) = 49 + 19.9 + Log_{10}(d)$ where the parameters of the classical power-law behavior have been estimated according to the measurement campaign.
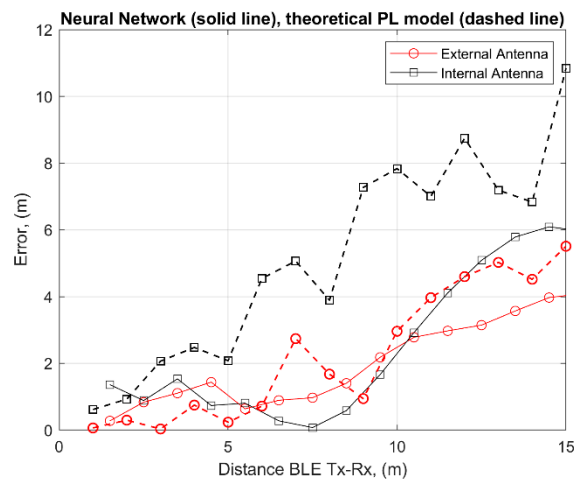
Figure 14. Error in distance estimation for external/internal antenna receivers for neural network (solid line) and theoretical pathloss model (dashed line).

6.2. Deployment of BLE Receivers and Accuracy Evaluation of the Localization Procedure

In this section we analyze the localization accuracy of the procedure. Furthermore, we also investigate the position and the number of BLE receivers to be deployed in the considered museum rooms. In Table 1, we described the scenarios involved in accuracy evaluation. In the experiment, we varied the number and position of the BLE receivers in the area. Figure 15 reports the position of the BLE receivers. All receivers were placed at a height of approximately 1.5 m from the ground.

Table 1. Definition of the considered scenarios.

Scenario	Receiver Position	Receiver Type
Scenario 1	BLE receivers located in positions A	Four receivers with external antenna
Scenario 2	BLE receivers located in positions A	Four receivers with internal antenna
Scenario 3	BLE receivers located in positions B	Four receivers with external antenna
Scenario 4	BLE receivers located in positions B	Four receivers with internal antenna
Scenario 5	BLE receivers located in positions A	Two receivers with internal antenna (dashed) Two receivers with external antenna (solid)
Scenario 6	BLE receivers located in positions B	Two receivers with internal antenna (dashed) Two receivers with external antenna (solid)
Scenario 7	BLE receivers located in positions C	Five receivers with internal antenna (dashed) Four receivers with external antenna (solid)

To evaluate the accuracy of the position procedure we selected eight possible positions (Xreal, Yreal) of the transmitter in the area reported in Table 2. The NLS algorithm solves non-linear problems given a number of receivers greater than or equal to three in known positions. It is therefore required that the array with the distance estimate is composed of at least three elements. Theoretically, if the distance array is composed of only three elements (no fewer), the trilateration algorithm provides even in this case a distance estimate, but with reduced accuracy.
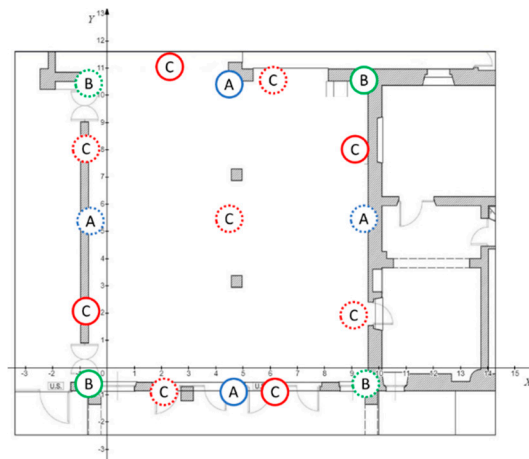
Figure 15. Positions of the BLE receivers in the scenarios considered for localization procedure.

Table 2. Errors in position estimate according to the considered deployment strategies: average and standard deviation of the error for each scenario are in bold.

Test nr	Xreal	Yreal	Scen. 1 Error (m)	Scen. 2 Error (m)	Scen. 3 Error (m)	Scen. 4 Error (m)	Scen. 5 Error (m)	Scen. 6 Error (m)	Scen. 7 Error (m)
1	1	7	5.75	1.73	2.63	0.71	4.07	1.79	1.00
2	2	2	5.51	3.74	1.95	4.14	1.77	1.82	0.41
3	2	8	4.91	2.74	2.73	1.70	4.63	2.40	0.37
4	3	2	0.81	4.07	3.74	2.93	0.40	3.28	0.70
5	3	3	5.76	1.97	0.35	1.49	0.67	1.35	1.21
6	3	4	4.78	1.19	2.01	1.66	1.20	1.10	1.00
7	4	6	0.94	1.17	2.95	2.11	1.96	0.95	1.53
8	4	8	0.64	3.14	3.89	1.54	2.27	3.24	0.45
9	1	4	1.63	1.49	3.12	1.07	0.56	1.93	1.13
10	2	5	3.96	1.35	3.42	1.78	1.12	1.21	0.64
11	2	7	5.16	2.57	2.65	2.69	4.37	2.21	0.89
12	3	9	5.83	3.79	2.41	1.34	3.56	3.08	0.90
13	4	3	4.83	2.14	3.25	1.37	0.78	1.09	1.44
14	5	8	0.78	3.25	2.78	2.82	1.78	2.99	0.42
15	5	4	2.20	2.35	0.78	3.47	2.45	1.43	0.57
Avg. error (m)			**3.57**	**2.45**	**2.58**	**2.05**	**2.11**	**1.99**	**0.84**
Error Std Dev. (m)			**2.11**	**0.98**	**0.99**	**0.96**	**1.43**	**0.83**	**0.38**

Table 2 also reports the results of the position estimations from the localizer (Xestimated, Yestimated) for the considered deployment scenarios described in Table 1.

The average accuracy was between 2 and 3.6 m in cases where only four receivers were deployed in the museum room according to the strategies in Figure 15. In order to improve the accuracy of the position of the visitor in a room of the museum we increased the number of BLE receivers according to scenario 7. In the event, it provided a reduced estimation error of 84 cm. In this configuration, the external antenna receivers guaranteed, in accordance with the radiation diagram, good coverage in the north-south direction even beyond 4 m, while those with an integrated antenna compensated for the lack of coverage in the narrowest corners of the radiation beam, although with a limited range of action of approximately 4 m. Table 2 also reports the average error and its standard deviation for each considered scenario.

Figure 16 reports the cumulative distribution function (CDF) of the errors in position estimation for the considered scenarios. It allows easy visualization of the non-overcome error for a given percentage in order to assess the reliability of the localization system in the scenarios. For example, in scenario 5 the localization system guaranteed an error lower than 4.35 m in 90% of the cases, while it guaranteed an error lower than 1.45 m in 90% of the cases in scenario 7.
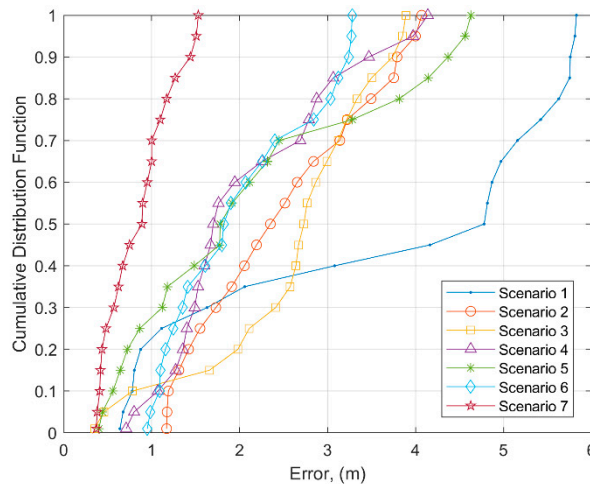
Figure 16. Cumulative distribution function (CDF) of the errors for the different scenarios of Figure 15.

Due to the introduction of greater errors in cases of considering more than three receivers (i.e., the closest), Figure 17 reports the error in the position estimate when all receivers are considered in the NLS algorithm.
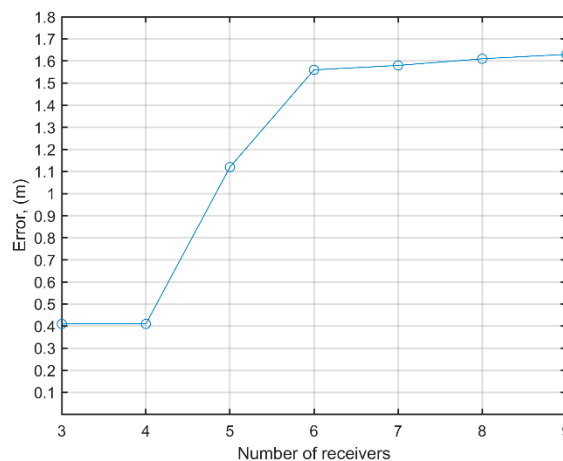

Figure 17. Relationship between number of receivers and error.

The results show that an increase in the considered receivers (and then in the estimated distances) provides greater errors in the position estimate. This means that the distance estimate for receivers far from the transmitter has high errors that reduce the accuracy of the procedure.

As a final result, we considered the fact that in museums the one or two best receivers (according to the ordering obtained without humans in the room) can be obstructed by the presence of visitors. To take into account any possible human obstruction, we assumed the RSSI received by the obstructed receivers to be considered under the SNR threshold (worst case), thus not allowing the localizer to exploit its measurement sets. To evaluate these cases, we repeated the estimates by eliminating one or two distance estimates provided by the best receivers. In case of one obstructed receiver (i.e., 33%, since the NLS algorithm considers the best three estimates), we supposed eliminating one of the three best receivers and adding the fourth best receiver for the position estimate, according to the order in which they performed. We averaged this procedure for the three best receivers and for the fifteen transmitter positions reported in Table 2. We also considered the case of obstruction of two of the three best receivers corresponding to 66%. In this case, we needed to consider the fifth best receiver for the position algorithm. We considered scenario 7 and the results are reported in Table 3. In the obstructed cases, the error increased to about 1.6 m and 1.8 m.

Table 3. Errors in position estimate when one (33%) or two (66%) obstructions of the best three receivers occur for scenario 7: average and standard deviation of the error for each scenario are in bold.

Nr.	Xreal	Yreal	Xestimated	Yestimated	Error (m)	Avg. Error 33% Obstruction (m)	Avg. Error 66% Obstruction (m)
1	1	7	1.83	7.56	1.00	2.54	2.47
2	2	2	2.04	2.41	0.41	0.86	1.57
3	2	8	2.21	7.7	0.37	2.65	2.49
4	3	2	2.74	2.65	0.70	2.62	2.29
5	3	3	1.96	3.62	1.21	1.81	1.80
6	3	4	3.53	3.15	1.00	0.60	0.91
7	4	6	2.72	6.83	1.53	0.66	1.27
8	4	8	4.26	8.37	0.45	0.83	1.79
9	1	4	1.78	4.82	1.13	2.01	2.31
10	2	5	2.12	5.63	0.64	1.19	1.34
11	2	7	2.28	7.85	0.89	1.58	1.76
12	3	9	2.82	8.12	0.90	2.09	1.92
13	4	3	2.6	2.67	1.44	2.76	2.97
14	5	8	4.69	8.29	0.42	0.58	1.09
15	5	4	5.12	4.56	0.57	0.97	1.66
Avg. error (m)					**0.84**	**1.58**	**1.84**
Error Std Dev. (m)					**0.38**	**0.82**	**0.58**

In Figure 18 we report the CDF of the errors in position estimation for scenario 7 when human obstruction is considered. In both cases (33% and 66%), the localization system was able to guarantee an error lower than about 2.5 m in 90% of cases.
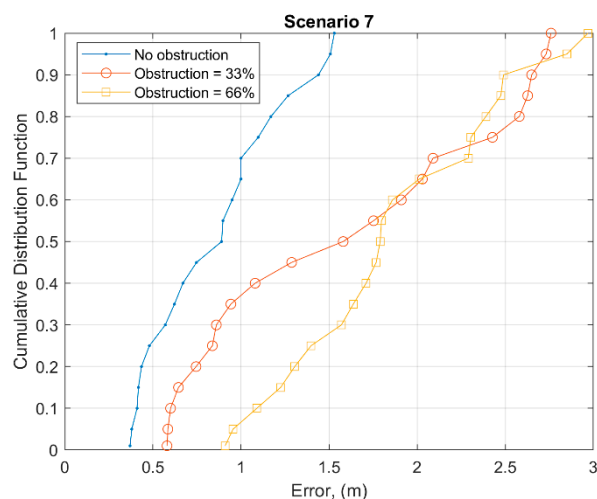

Figure 18. CDF of the errors in case of human obstruction for scenario 7.

7. Conclusions

The positioning of people indoors is an important topic when seeking to provide a complete user experience in some environments such as museums. In this paper we proposed a complete system for the indoor localization of people. According to the considered system architecture, the transmitter and the receivers adopt BLE technology. Then, the collected data are sent to a data store via Wi-Fi exploiting the MQTT protocol. Data are then filtered/ordered and a localizer estimates the position of the transmitter by the NLS algorithm. To characterize the environment, we performed a measurement campaign whose data were used to train a neural network. We also modeled the receiver antennas.

Moreover, we considered some deployment strategies for the receivers in the museum room. The accuracy of the position estimate was in the order of 2 m but could be improved to lower than 1 m when the number of BLE receivers was increased. Finally, we also evaluated the impact of obstruction caused by the presence of many visitors in the museum.

As a future improvement of this work, a finer analysis of human obstruction can be considered; for example, by trying to estimate the presence of a person through another neural network. This neural network could be used to dynamically measure the RSSI. When a human obstruction is detected the receiver can thus be properly used in the position estimate instead of discarded.

References

1. Zafari, F.; Gkelias, A.; Leung, K.K. A Survey of Indoor Localization Systems and Technologies. *IEEE Commun. Surv. Tutor.* **2019**, *21*, 2568–2599. [CrossRef]

2. Raza, U.; Kulkarni, P.; Sooriyabandara, M. Low Power Wide Area Networks: An Overview. *IEEE Commun. Surv. Tutor.* **2017**, *19*, 855–873. [CrossRef]

3. Darroudi, S.M.; Gomez, C. Bluetooth Low Energy Mesh Networks: A Survey. *Sensors* **2017**, *17*, 1467. [CrossRef] [PubMed]

4. Aggarwal, C.; Han, J. A survey of RFID data processing. In *Managing and Mining Sensor Data*; Springer Science: New York, NY, USA, 2013; pp. 349–382. ISBN 9781461463092.

5. Ferroni, P.; Zanzotto, F.M.; Riondino, S.; Scarpato, N.; Guadagni, F.; Roselli, M. Breast cancer prognosis using a machine learning approach. *Cancers* **2019**, *11*, 328. [CrossRef]

6. Ferroni, P.; Zanzotto, F.M.; Scarpato, N.; Riondino, S.; Guadagni, F.; Roselli, M. Validation of a machine learning approach for venous thromboembolism risk prediction in oncology. *Dis. Markers* **2017**, *2017*, 1–7. [CrossRef]

7. Matta, M.; Cardarilli, G.C.; Di Nunzio, L.; Fazzolari, R.; Giardino, D.; Nannarelli, A.; Re, M.; Spanò, S. A reinforcement learning based QAM/PSK symbol synchronizer. *IEEE Access* **2019**, *7*, 124147–124157. [CrossRef]

8. Beritelli, F.; Capizzi, G.; Lo Sciuto, G.; Napoli, C.; Woźniak, M. A novel training method to preserve generalization of RBPNN classifiers applied to ECG signals diagnosis. *Neural Netw.* **2018**, *108*, 331–338. [CrossRef]

9. Beritelli, F.; Capizzi, G.; Lo Sciuto, G.; Napoli, C.; Scaglione, F. Rainfall Estimation Based on the Intensity of the Received Signal in a LTE/4G Mobile Terminal by Using a Probabilistic Neural Network. *IEEE Access* **2018**, *6*, 30865–30873. [CrossRef]

10. Luna-Perejón, F.; Domínguez-Morales, M.; Gutiérrez-Galán, D.; Civit-Balcells, A. Low-Power Embedded System for Gait Classification Using Neural Networks. *J. Low Power Electron. Appl.* **2020**, *10*, 14. [CrossRef]

11. Spanò, S.; Cardarilli, G.C.; Di Nunzio, L.; Fazzolari, R.; Giardino, D.; Nannarelli, A.; Matta, M.; Re, M. An Efficient Hardware Implementation of Reinforcement Learning: The Q-Learning Algorithm. *IEEE Access* **2019**, *7*, 186340–186351.

12. Losh, M.; Llamocca, D. A low-power spike-like neural network design. *Electron. Switz.* **2019**, *8*, 1479. [CrossRef]

13. Cardarilli, G.C.; Di Nunzio, L.; Fazzolari, R.; Nannarelli, A.; Re, M.; Spano, S. N-Dimensional Approximation of Euclidean Distance. *IEEE Trans. Circuits Syst. Express Briefs* **2020**, *67*, 565–569. [CrossRef]

14. Giuliano, R.; Mazzenga, F.; Petracca, M.; Vatalaro, F. Application of Radio Frequency Identification for Museum Environment. In Proceedings of the Workshops on Enabling Technologies: Infrastructure for Collaborative Enterprises, Hammamet, Tunisia, 17–20 June 2013; pp. 190–195.

15. Danis, F.S.; Cemgil, A.T. Model-Based Localization and Tracking Using Bluetooth Low-Energy Beacons. *Sensors* **2017**, *17*, 2484. [CrossRef] [PubMed]

16. Sthapit, P.; Gang, H.; Pyun, J. Bluetooth Based Indoor Positioning Using Machine Learning Algorithms. In Proceedings of the IEEE International Conference on Consumer Electronics, Asia (ICCE-Asia), Jeju, Korea, 24–26 June 2018; pp. 206–212. [CrossRef]

17. Nurminen, H.; Dashti, M.; Piché, R. A Survey on Wireless Transmitter Localization Using Signal Strength Measurements. *Wirel. Commun. Mobile Comput.* **2017**. [CrossRef]

18. Chiou, S.-Y.; Liao, Z.-Y. Design and Implementation of Beacon-Based Positioning. *J. Inf. Sci. Eng.* **2020**, *36*, 643–658. [CrossRef]

19. Lohan, E.-S.; Talvitie, J.; Figueiredo De Silva, P.; Nurminen, H.; Ali-Löytty, S.; Piche, R. Received Signal Strength models for WLAN and BLE-based indoor positioning in multi-floor buildings. In Proceedings of the International Conference on Localization and GNSS (ICL-GNSS), Gothenburg, Sweden, 22–24 June 2015. [CrossRef]

20. Zuo, Z.; Liu, L.; Zhang, L.; Fang, Y. Indoor Positioning Based on Bluetooth Low-Energy Beacons Adopting Graph Optimization. *Sensors* **2018**, *18*, 3736. [CrossRef]

21. Kriz, P.; Maly, F.; Kozel, T. Improving Indoor Localization Using Bluetooth Low Energy Beacons. *Mobile Inf. Syst.* **2016**, 11. [CrossRef]

22. Ishida, S.; Takashima, Y.; Tagashira, S.; Fukuda, A. Proposal of Separate Channel Fingerprinting Using Bluetooth Low Energy. In Proceedings of the 5th IIAI International Congress on Advanced Applied Informatics (IIAI-AAI), Kumamoto, Japan, 10–14 July 2016; pp. 230–233.

23. Hoang, M.T.; Yuen, B.; Dong, X.; Lu, T.; Westendorp, R.; Reddy, K. Recurrent Neural Networks for Accurate RSSI Indoor Localization. *IEEE Internet Things J.* **2019**, *6*, 10639–10651. [CrossRef]

24. Mackin, C. *Exploration for Range Based Indoor Localization Technologies and Algorithms*; Technical Report No. UCB/EECS-2018-109; Electrical Engineering and Computer Sciences University of California: Berkeley, CA, USA, August 2018; Available online: http://www2.eecs.berkeley.edu/Pubs/TechRpts/2018/EECS-2018-109.html (accessed on 9 August 2018).

25. Gu, Y.; Lo, A.; Niemegeers, I. A survey of indoor positioning systems for wireless personal networks. *IEEE Commun. Surv. Tutor.* **2009**, *11*, 13–32. [CrossRef]

26. Yang, J.; Li, Y.; Cheng, W. An improved geometric algorithm for indoor localization. *Int. J. Distrib. Sens. Netw.* **2018**, *14*, 1–13. [CrossRef]

27. Mussina, A.; Aubakirov, S. RSSI Based Bluetooth Low Energy Indoor Positioning. In Proceedings of the IEEE 12th International Conference on Application of Information and Communication Technologies (AICT), Almaty, Kazakhstan, 17–19 October 2018; pp. 1–4.

28. Hillar, C.C. *MQTT Essentials—A Lightweight IoT Protocol*; Packet Publishing: Birmingham, UK, 2017.

29. Xu, B.; Zhu, X.; Zhu, H. An Efficient Indoor Localization Method Based on the Long Short-Term Memory Recurrent Neuron Network. *IEEE Access* **2019**, *7*, 123912–123921. [CrossRef]

30. Naghdi, S.; O'Keefe, K. Detecting and Correcting for Human Obstacles in BLE Trilateration Using Artificial Intelligence. *Sens. Basel* **2020**, *20*, 1350. [CrossRef] [PubMed]

31. Dinh, T.T.; Duong, N.; Sandrasegaran, K. Smartphone-based Indoor Positioning Using BLE iBeacon and Reliable Lightweight Fingerprint Map. *IEEE Sens. J.* **2020**. [CrossRef]

32. Iqbal, Z.; Luo, D.; Henry, P.; Kazemifar, S.; Rozario, T.; Yan, Y.; Westover, K.; Lu, W.; Nguyen, D.; Long, T.; et al. Accurate real time localization tracking in a clinical environment using Bluetooth Low Energy and deep learning. *PLoS ONE* **2018**, *13*, e0205392. [CrossRef] [PubMed]

33. Mazan, F.; Kovarova, A. A Study of Devising Neural Network Based Indoor Localization Using Beacons: First Results. *Comput. Inf. Syst. J.* **2015**, *19*, 15–20.

34. Tsitsipa, V.; Achillias, G.; Parthenios, P. Using big data to design user-centric museums. From visitors loyal to museums to museums loyal to users. In Proceedings of the Education and Research in Computer Aided Architectural Design in europe (eCAADe), Łódź, Poland, 19–21 September 2018.

35. Bluetooth Smart or Version 4.0+ of the Bluetooth Specification. Available online: bluetooth.com (accessed on 10 March 2017).

36. Hernández-Rojas, D.L.; Fernández-Caramés, T.M.; Fraga-Lamas, P.; Escudero, C.J. Design and Practical Evaluation of a Family of Lightweight Protocols for Heterogeneous Sensing through BLE Beacons in IoT Telemetry Applications. *Sensors* **2018**, *18*, 57. [CrossRef]

37. Espressif Systems, ESP32-WROOM-32D & ESP32-WROOM-32U Datasheet v1.9. Available online: https://www.espressif.com/sites/default/files/documentation/esp32-wroom-32d_esp32-wroom-32u_datasheet_en.pdf. (accessed on 9 June 2020).

38. SR Passives, Wi-Fi—Ant 410-1. Available online: https://www.tme.eu/Document/c80a7d27e7324afe40b4ab4d29f42817/WIFI-ANT410-1.pdf (accessed on 9 June 2020).

39. Goldoni, E.; Savioli, A.; Risi, M.; Gamba, P. Experimental analysis of RSSI-based indoor localization with IEEE 802.15.4. In Proceedings of the European Wireless Conference (EW), Lucca, Italy, 12–15 April 2010; pp. 71–77.

40. Capizzi, G.; Coco, S.; Lo Sciuto, G.; Napoli, C. A New Iterative FIR Filter Design Approach Using a Gaussian Approximation. *IEEE Signal. Process. Lett.* **2018**, *25*, 1615–1619. [CrossRef]

41. Murphy, W.S.; Hereman, W. *Determination of a Position in Three Dimensions Using Trilateration and Approximated Distances*; Technical Report MCS-95-07; Colorado School of Mines: Golden, CO, USA, October 1995; pp. 1–19. Available online: https://inside.mines.edu/~{}whereman/papers/Murphy-Hereman-Trilateration-MCS-07-1995.pdf (accessed on 9 June 2020).